NASA Technical Memorandum 86777

USAAVSCOM Technical Report 85-A-06

NASA-TM-86777

19860002740

Some Recent Advances in Computational Aerodynamics for Helicopter Applications

W.J. McCroskey and J.D. Baeder

October 1985

NF00040

NASA

National Aeronautics and
Space Administration

United States Army
Aviation Systems
Command

Some Recent Advances in Computational Aerodynamics for Helicopter Applications

W J. McCroskey,
J D. Baeder,   Aeroflightdynamics Directorate, U. S. Army Research
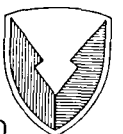   and Technology Activity-AVSCOM, Moffett Field, California

October 1985

N86-12207

SOME RECENT ADVANCES IN COMPUTATIONAL AERODYNAMICS FOR HELICOPTER APPLICATIONS*

W. J. McCroskey and J. D. Baeder
U.S. Army Aeroflightdynamics Laboratory (AVSCOM)
NASA Ames Research Center, Moffett Field, California 94035 USA

ABSTRACT

The growing application of computational aerodynamics to nonlinear helicopter problems is outlined, with particular emphasis on several recent quasi-two-dimensional examples that used the thin-layer Navier-Stokes equations and an eddy-viscosity model to approximate turbulence. Rotor blade section characteristics can now be calculated accurately over a wide range of transonic flow conditions. However, a finite-difference simulation of the complete flow field about a helicopter in forward flight is not currently feasible, despite the impressive progress that is being made in both two and three dimensions. The principal limitations are today's computer speeds and memories, algorithm and solution methods, grid generation, vortex modeling, structural and aerodynamic coupling, and a shortage of engineers who are skilled in both computational fluid dynamics and helicopter aerodynamics and dynamics.

I. INTRODUCTION

The flow fields around rotating helicopter blades provide a rich variety of challenging problems in applied computational aerodynamics. As illustrated schematically in the lower right corner of figure 1, the flow is three dimensional and unsteady, with periodic regions of transonic flow near the blade tips, and includes inboard dynamic stall pockets. The blades also shed complex vortical wakes, and the concentrated tip vortex of each blade generally passes close to successive blades. Furthermore, even on the most modern, streamlined helicopters, complicated aerodynamic interactions arise between the major components, such as the main rotor, hub, fuselage, and tail rotor.

For many years, helicopter engineers have used a mixture of simplified linear aerodynamic theories, wind tunnel data, and design charts; whereas a small community of research scientists has systematically explored the details of individual pieces of the overall problem, as indicated by the sketches in figure 1. References 1 and 2 provide an overall picture of the practical side, and references 2 and 3 summarize many of the recent studies of these simpler "building blocks." It is significant that, despite the large gap between the two-dimensional blocks and the real world, the helicopter industry still relies heavily on two-dimensional airfoil

---
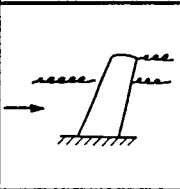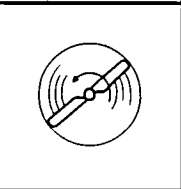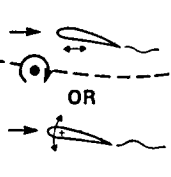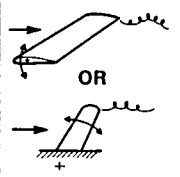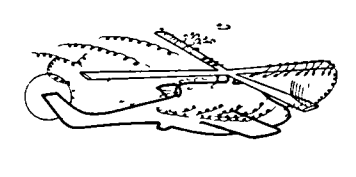
	2 DIM	3-D (NONROTATING)	3-D (ROTATING)	3 D FORWARD FLIGHT
STEADY				
UNSTEADY	OR	OR		

Fig. 1 Development of rotor blade aerodynamics from simpler cases.

characteristics. Figure 2 shows the approximate blade-element environment and airfoil requirements for modern high-speed rotors. Although the operational Mach numbers for helicopter airfoils are less than one, transonic flow often develops over a large fraction of the rotor disc because of the combined rotational and translational velocities, angles of attack, or blade-vortex interactions.

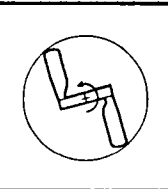This paper selectively reviews some recent advances in computational fluid dynamics that are relevant to helicopter aerodynamics. Especially in the two-dimensional, transonic flow regime, numerical studies using supercomputers can already complement or replace the extensive wind tunnel testing that has traditionally been the main source of helicopter airfoil data. Several recent investigations[4-10] have helped to highlight the challenges, capabilities, and limitations of future, more ambitious efforts, and they enable some projections to be made regarding the potential of computational aerodynamics for realistic helicopter applications.

II. STEADY TWO-DIMENSIONAL AIRFOIL CALCULATIONS

As indicated in figure 2, the "advancing" blade tip operates in a complex transonic environment, where the rotor blades' aerodynamic section characteristics, such as lift, drag, and pitching-moment coefficients, differ substantially from even the qualitative behavior of subsonic airfoils. In reference 4, the NASA Ames code ARC2D (Refs. 11,12) was used to calculate the transonic viscous flow of several helicopter profiles. This code uses an alternating-direction fully implicit (ADI), approximate-factorization scheme to solve the thin-layer Reynolds-averaged Navier-Stokes equations, with an algebraic eddy-viscosity model[13] to approximate boundary-layer turbulence. Approximately 90 combinations of airfoil geometry, Mach
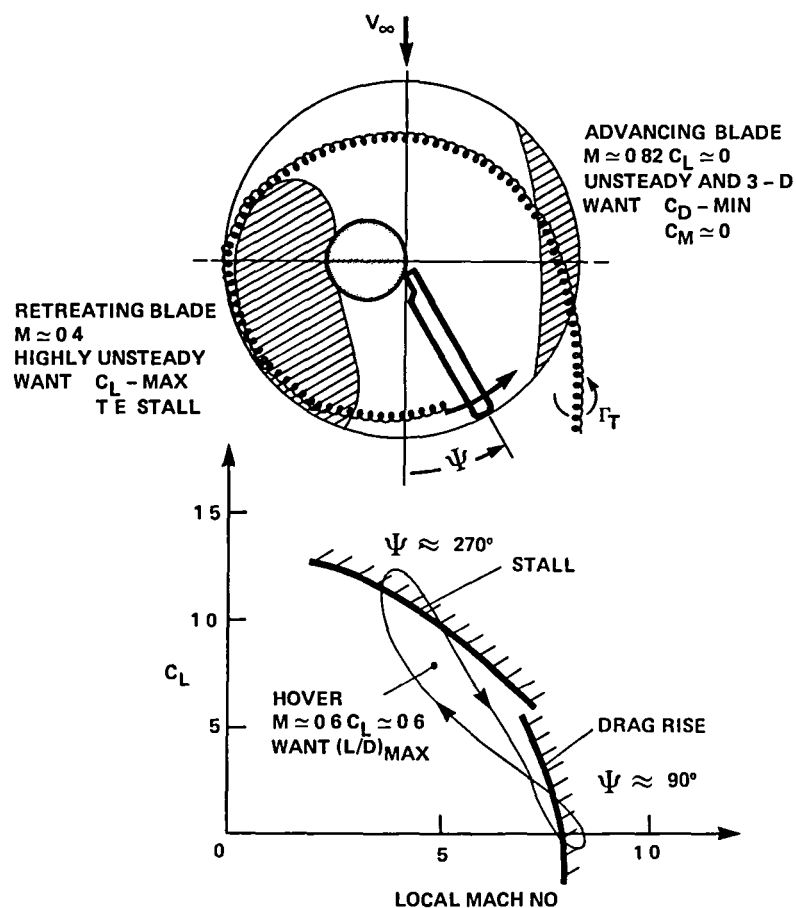
Fig. 2 Helicopter airfoil requirements for hover and forward flight.

number, Reynolds number, and angle of attack were computed, in what is believed to be the first attempt to apply such a sophisticated code to a wide range of practical airfoil cases. The details of the numerical method, including the governing equations, boundary conditions, computational grids, convergence characteristics, and estimated accuracy, are given in reference 4 and 11-13.

Figures 3-5 show representative results for combinations of Mach numbers and angles of attack that produce significant nonlinear behavior and shock wave-boundary layer interaction. In these examples, the boundary layer is assumed to be turbulent downstream of x/c = 0.01. Body-conforming C-type grids were used, with 193 points around the airfoil and 64 points in the normal direction. The typical CPU time for each case was approximately 10 min on the Ames Cray X-MP computer, although the solutions generally converged to within the estimated overall numerical-accuracy bounds within approximately 7 min.

As shown in the figures, the numerical results reproduce the experimentally observed airfoil behavior across the transonic regime, from low subsonic to supersonic, with an accuracy that is comparable to what is typically obtained in the wind

3
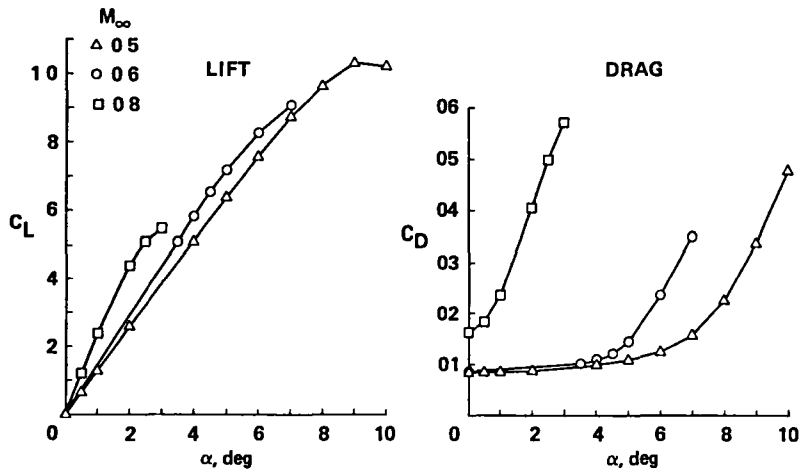
Fig. 3   Calculated results for the NACA 0012 airfoil with leading-edge trip;
Re = 6 × 10^6.
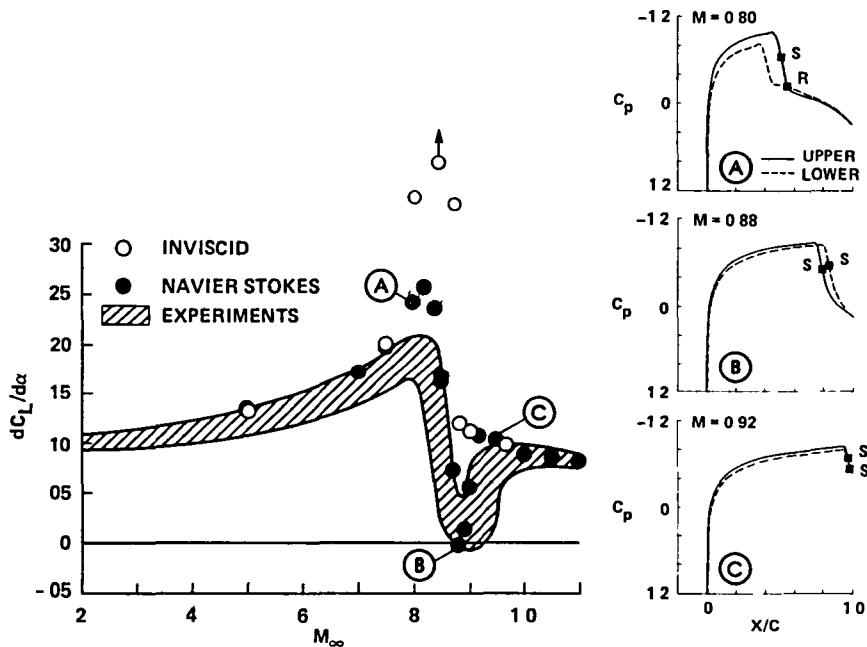
Fig. 4   Transonic characteristics of the NACA 0012 airfoil.

tunnels. Also, the details of the computed flow fields provide new insights into
transonic airfoil behavior under conditions for which accurate measurements are
difficult to obtain, and which are often tainted significantly by wall-interference
effects.

Figure 4 shows $dC_L/d\alpha$ vs Mach number; that is, the lift behavior at low
angles of attack, including the loss of lift that occurs when significant separation
is induced by the shock waves. This phenomenon occurs for $0.83 < M_\infty < 0.93$ for the
NACA 0012 airfoil, with the minimum lift occurring at $M_\infty \approx 0.88 - 0.90$.
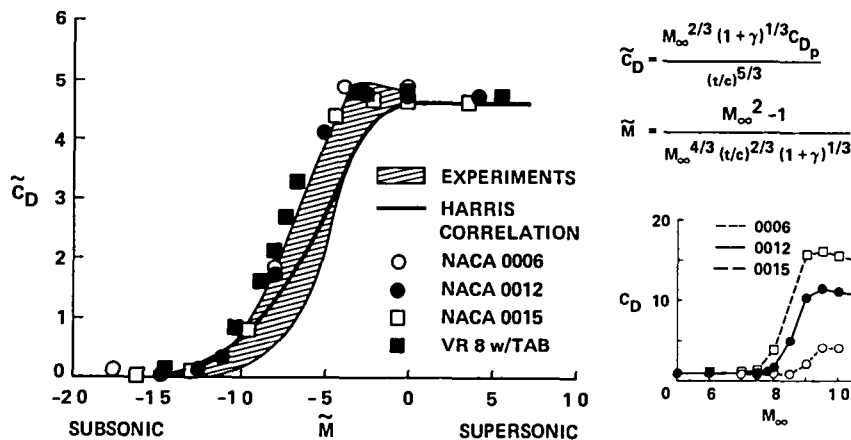
Fig. 5 Correlation of drag calculations in transonic similarity parameters.

The computed pressure distributions and separation-point locations, as given on the right side of figure 4, show how the transonic loss of lift occurs and how the lift recovers when the shock waves move to the trailing edge at the higher Mach numbers. The open symbols in figure 4 show inviscid results, which do not predict the transonic dip and which are clearly inadequate in this range of Mach number.

The drag rise in the transonic regime is shown in figure 5, both as C_D vs M_∞ and as the similarity parameters $\tilde{C}_D$ vs $\tilde{M}$, where C_{D_P} is the increment in drag coefficient above the subsonic, zero-lift value. The Harris correlation and the airfoil shapes are discussed in reference 4. Especially noteworthy is the collapse of the computed results for four different airfoils across a Mach-number range spanning the entire transonic regime to virtually a single curve of $\tilde{C}_D$. It should also be mentioned that there is considerable scatter in the available measurements, with the results for a given airfoil for C_D from different wind tunnels differing more than the results for different airfoils in the same wind tunnel (cf. Ref. 4).

Other airfoil characteristics of interest to helicopter engineers, such as the maximum lift-to-drag ratios, the transonic pitching-moment behavior,and the effects of Reynolds number between 10^6 and 10^8, were also calculated and presented in reference 4. In all cases, the calculated results correlated well and agreed with the available measurements to within the scatter of the wind tunnel data. However, retreating-blade stall has been avoided up to now, because of the difficulties and uncertainties regarding turbulence modeling and massive flow separation. But otherwise, this use of computational aerodynamics can now be considered a viable tool for determining helicopter airfoil characteristics.

III. UNSTEADY AIRFOIL-VORTEX INTERACTION

The interaction of a rotor blade with the concentrated tip vortices which are trailed by other blades can be an important source of unsteady airloads and noise. This phenomenon is especially important on the advancing blade, and in cases where

the angle between the axis of the vortex and leading edge of the blade is small. As this intersection angle approaches zero, the problem can be modeled in two dimensions; namely, as a concentrated vortex convecting past a quasi-stationary airfoil.

Unsteady transonic calculations of this model problem have been performed[5] using an inviscid small-disturbance code and a special variation of the ARC2D code mentioned above, in both the Euler and the thin-layer Navier-Stokes modes. In all cases, a special form of vortex fitting has been employed to introduce concentrated vortical disturbances into the computational domain; otherwise, numerical dissipation alters the vortex structure and erroneously weakens the interaction. The basic scheme is to split the solution vector $\vec{q}$ into two parts, $\vec{q} = \vec{q}_A + \vec{q}_v$ where $\vec{q}_v$ represents the prescribed structure of the vortex, such as a Lamb-like velocity distribution

$$V_\theta = \frac{\Gamma_v}{2\pi r} \left(1 - e^{-r^2/a^2} \right) \tag{1}$$

that convects with the flow past the airfoil, and $\vec{q}_A$ is the remaining part of the solution that is due to the presence of the airfoil. The resulting nonlinear equation, or set of equations, for $\vec{q}_A = \vec{q} - \vec{q}_v$ is solved subject to the appropriate boundary conditions for $\vec{q}$. The details of the procedure are given in Refs. 5 and 14; the viscous scheme was recently upgraded to include the adaptive-grid method of Nakahashi and Deiwert,[15] as discussed in Ref. 5. For a 221 × 67 C-type body-conforming grid, the CPU time on the Ames Cray X-MP computer was approximately 20 min for the initial or steady-state solution without the vortex, and approximately 40 additional minutes for the calculation of the unsteady interaction as the vortex convected past the airfoil.

Results for a Stationary Rotor Airfoil. For representative helicopter conditions, the airfoil-vortex interaction problem is strongly influenced by transonic effects, but it is less sensitive to viscous effects than are the examples in figures 3-5. The dominant features of this flow are illustrated in figure 6 (adapted from Ref. 5), for a stationary, symmetrical airfoil at zero incidence, and whose boundary layer is turbulent from the leading edge. In this case, the vortex has a circulation with a clockwise sense; therefore, when the vortex is ahead of the airfoil, it induces a time- and spatially dependent "downwash," or negative angle of attack, on the airfoil. This changes to an "upwash" as the vortex convects past the trailing edge.

The upper part of figure 6 shows the instantaneous pressure distributions corresponding to four instantaneous locations of the moving vortex. Since the flow past the airfoil is symmetrical in the absence of the airfoil, the differences between the upper and lower surfaces are due solely to the interaction with the vortex. The middle part of the figure shows the grid as it adapts to each step of the calculation. The fine resolution near the shock waves enables details in the flow field to be captured that were not evident in earlier fixed-grid solutions.

6

PRESSURE DISTRIBUTION

$x_v = 0$ $x_v = 0.2$ $x_v = 0.5$ $x_v = 1.0$

-1.2

C_p 0

C_p^* C_p^* C_p^* C_p^*

-- UPPER
— LOWER

1.2 (a)   (b)   (c)   (d)

ADAPTIVE GRID

$.6$ $x_v = 0$ $x_v = 0.2$ $x_v = 0.5$ $x_v = 1.0$

y 0

$-.6$ (a)   (b)   (c)   (d)

$-.2$ x 1.0 $-.2$ x 1.0 $-.2$ x 1.0 $-.2$ x 1.0

PRESSURE CONTOURS

1 $x_v = 0$ $x_v = 0.2$ $x_v = 0.5$ $x_v = 1.0$

y 0

-1 (a)   (b)   (c)   (d)

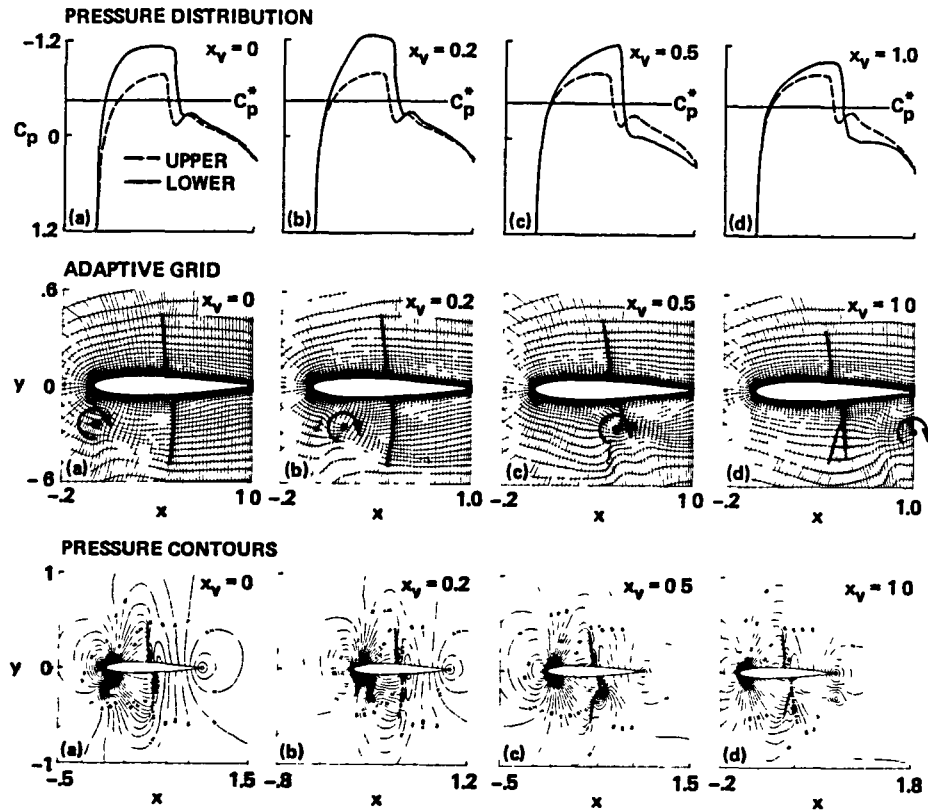$-.5$ x 1.5 $-.8$ x 1.2 $-.5$ x 1.5 $-.2$ x 1.8

Fig. 6 Instantaneous surface pressure distributions, adaptive grid, and pressure contours for airfoil-vortex interaction; NACA 0012, $M_\infty = 0.80$, $\alpha = 0$, $\Gamma_v = 0.20$, $y_v = -0.26$.

These details, such as the distortion of the lower-surface shock wave into a lambda pattern, show up in the pressure contours in the lower part of the figure.

Results for a Rotating Blade.- Unfortunately, there are few relevant experimental data with which to compare the above results, owing to the difficulty of creating a concentrated lateral vortex of the appropriate strength in a transonic wind tunnel. Also, most conventional helicopter rotor experiments lack the sufficient precision and documentation of the complete flow field that are necessary to validate the code in question. However, a recent landmark experiment by Caradonna et al.,[16] as shown in figure 7, provided measurements on a rotating blade that passed near a strong, concentrated vortex which was produced by a fixed wing that was placed upstream of the rotor model. The rotor blades were symmetrical and nonlifting in the absence of the upstream vortex generator, and the encounter occurred when the leading edge of the blade was parallel to the vortex. By this means, the measuring station on the blade, at 90% span, experienced approximately the type of interaction described above.

As discussed in reference 5, when the rotational speed of the model rotor was low enough for the flow to remain subcritical at all times, good agreement was obtained between the experimental and computed results. Typical results in this category are shown in figure 7. However, at the higher rotor tip speeds of the
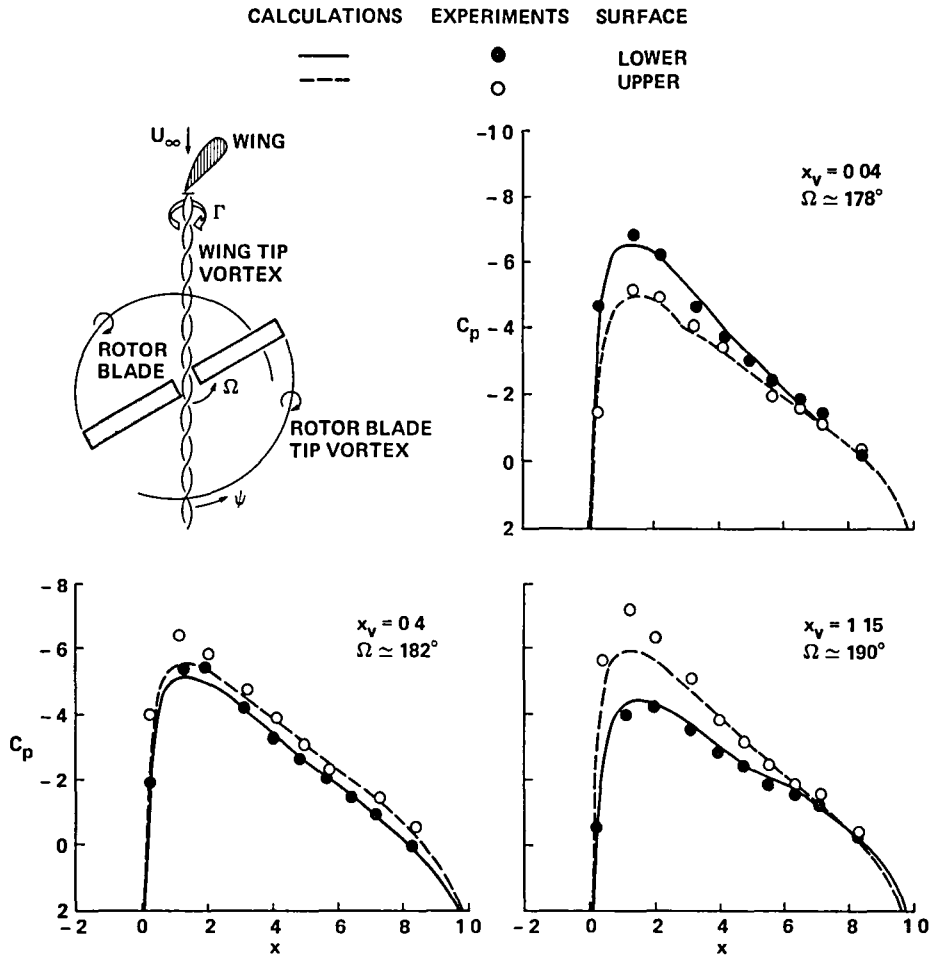
7

Fig. 7   Instantaneous pressure distributions for quasi-two-dimensional rotor-vortex interaction; M_T = 0.60, $U_\infty/\Omega R$ = 0.2, r/R = 0.893, Γ_V = 0.243, y_V = -0.40.

experiment, strong shock waves formed on the advancing blade, with or without the vortex, and these shock waves were found to almost totally dominate the experiment. Furthermore, the unsteady formation and decay of these shock waves were found to be highly dependent upon three-dimensional crossflow effects, even though the subcritical case was quasi-two-dimensional. Therefore, the comparison of the highly transonic data with the results of the two-dimensional airfoil-vortex interaction codes was not satisfactory.

On the other hand, some important insights on the challenges for future computational methods are evident when attempts are made to correlate the calculations with the transonic data. For example, figure 8 shows several piecemeal approaches, as described in reference 5, in comparison with the rotor measurements. The two-dimensional, stationary airfoil computations (Fig. 8b), which were representative of the state-of-the-art in blade-vortex modeling when using the advanced finite-difference methods of early 1985, produce unsatisfactory results. This methodology was recently updated to allow for the time-dependent Mach number which approaches the rotor section, M_L = M_R(1 + μ' sin ψ) (Fig. 8c); however, the inclusion of this
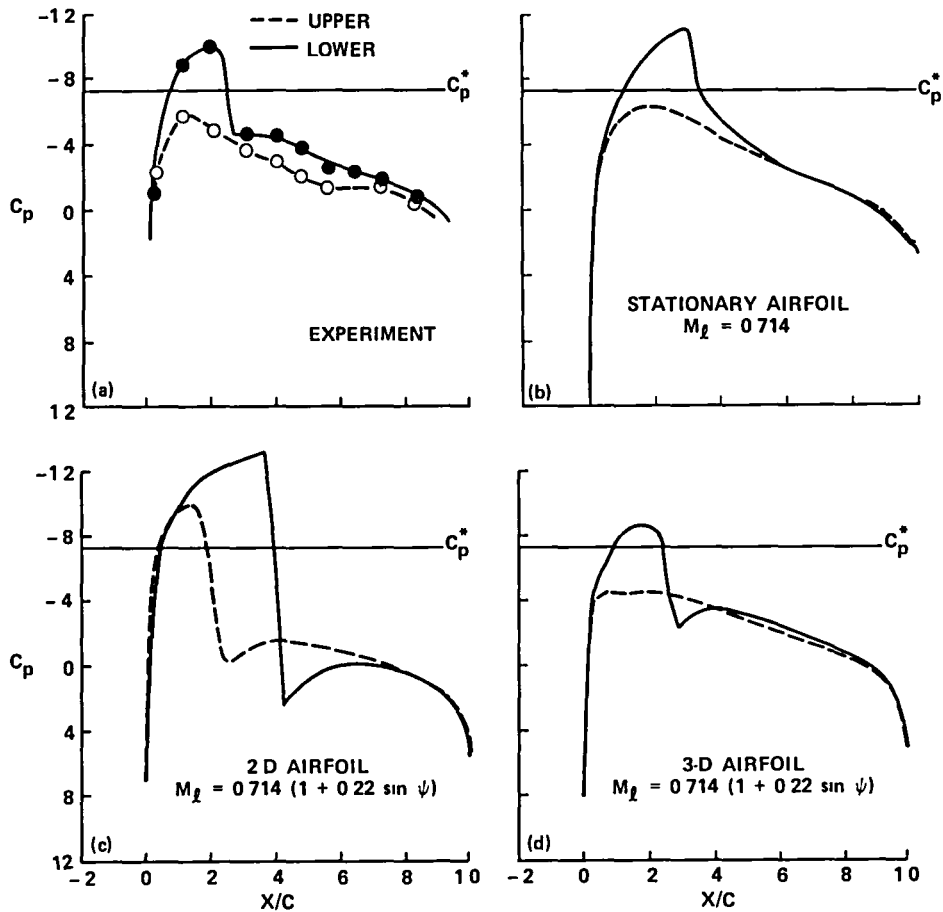
Fig. 8 Transonic rotor-vortex interaction; same conditions as Fig. 7 except $M_T = 0.80$.

effect <u>alone</u> is even less satisfactory. The inclusion of an ad hoc three-dimensional correction (Fig. 8d) gives much better agreement. However, as explained in Ref. 5, this correction is rather arbitrarily determined based on the rotor-alone solution, and, consequently, the calculations are not at all predictive. Rather, the comparisons shown in figures 7 and 8 make it clear that both three-dimensional <u>and</u> unsteady effects will generally have to be included in accurate predictions of blade-vortex interactions under transonic conditions.

<u>Acoustic Wave Propagation</u>. The final example of this section concerns the requirements for accurately calculating the propagation of pressure pulses away from an airfoil-vortex interaction. This problem was addressed recently by George and Chang,[17] using the transonic small-disturbance equations. They reported strong wave-propagation phenomena which they associated with Tijdeman's "Type C" shock wave motion.[18] That is, for some transonic conditions a shock wave is set into motion by the vortex interaction, and this shock wave moves upstream off the airfoil and into the oncoming flow. Their calculations indicated that this Type C

shock propagation was the predominant disturbance at distances of approximately
1 chord ahead of the airfoil, but that this phenomenon only occurred over a rela-
tively narrow range of conditions.

In particular, George and Chang reported that the pressure fluctuations ahead
of and below an NACA-64A006 airfoil changed significantly when the Mach number was
increased from 0.82 to 0.85. To examine this more closely, these two cases were
recomputed with a similar inviscid small-disturbance code, but with a much finer
grid (399 × 197), using 300 points ahead of the airfoil along the x-axis. These
results are shown in figure 9, where the top half of the figure shows the instanta-
neous pressure distributions on the lower surface of the airfoil at various stages
of the interaction. The present results and time-histories of the force coeffi-
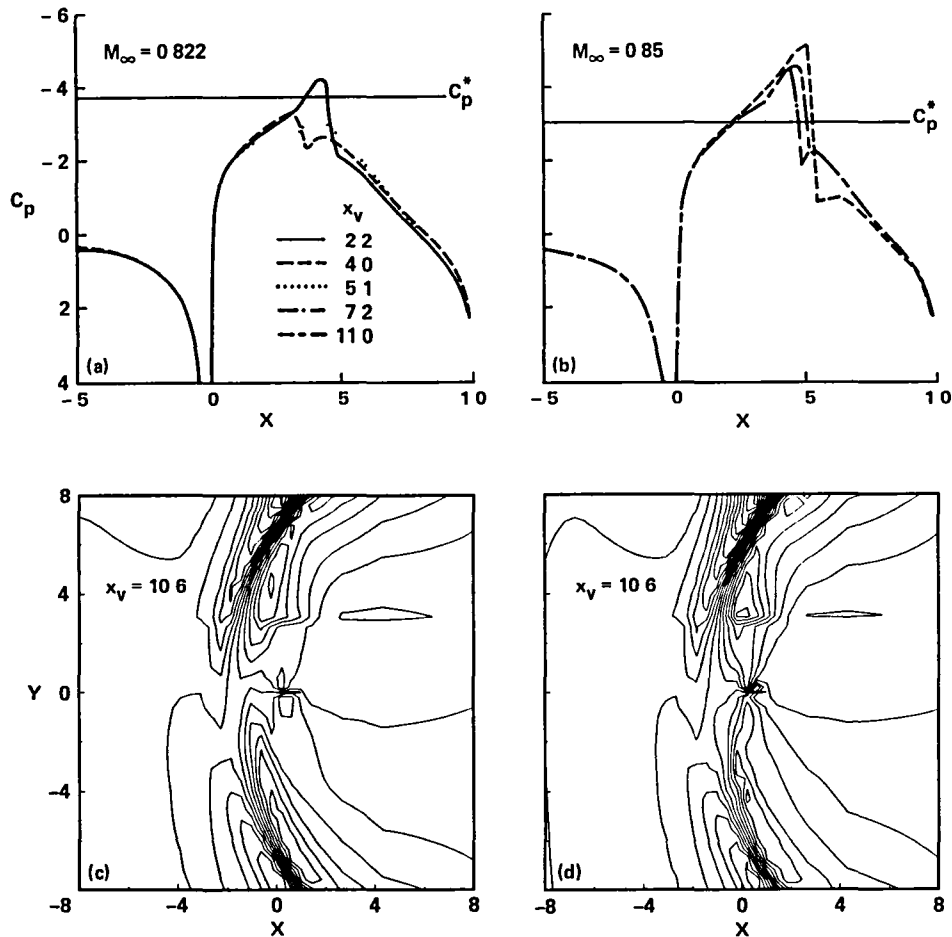cients (not shown) are in excellent agreement with those of George and Chang.

Fig. 9 Pressure distributions and acoustic wave propagation during airfoil-vortex
interaction; NACA 64A006 airfoil, Γ_v = 0.20, y_v = -0.26.

10

On the other hand, the lower part of figure 9 shows the perturbations in pressure relative to the pressure that is due to the airfoil alone in the absence of the vortex. Here the magnitudes of these fluctuating pressures are scaled by the square root of the distance from the leading edge, in accordance with the simple acoustic theory for the two-dimensional decay at large distances. This technique enables the far-field radiation to be more readily distinguished from the near-field disturbances, since the latter decay much faster with distance.

The interesting point about these fine-grid calculations is that the two separate cases seem remarkably similar in the "far field." There are some differences in the wave shapes and in other details, especially during the early stages of the airfoil-vortex encounter and close to the airfoil, and the magnitude of the pressure pulses along the x-axis seems to increase with increasing M_∞. However, nothing as fundamentally different as George and Chang's interpretations has been observed in our results. Rather, in both of these cases, and in numerous others, the major disturbance radiating to the far field appears to have a dipole characteristic that would be associated with the fluctuating lift. In any case, one of the major conclusions of this study is that much finer grids are required to resolve acoustic-propagation issues than for the airloads on the airfoil surface.

IV. PROJECTIONS FOR HELICOPTER CONFIGURATIONS

The lessons learned from the examples cited in section III clearly indicate that future helicopter applications will require three-dimensional adaptations of advanced computational techniques, that use suitably refined grids. Fortunately, this is the direction already in use by the fixed-wing airframe community, which remains which of the principal drivers of both large scientific computer technology and computational fluid-dynamics algorithm development. The helicopter industry will eventually benefit from advances made in fixed-wing aerodynamics, but there are important differences in the design and prediction requirements for the two types of aircraft that must be addressed. The special factors discussed below represent both major challenges and special opportunities for the next few years.

Unsteadiness is an important, complicating aspect of flows past rotor blades. This feature is shared by the aeroelasticity and turbomachinery communities, which have helped to extend the methodologies of quasi-steady aerodynamics, generally a few years after they were first introduced. However, existing time-accurate codes tend to have stability restrictions that restrict the time-steps to values which are much smaller than those which are necessary for accurate resolution of the relevant unsteady physics of the flow. As discussed in reference 19, such restrictions increase the CPU time by an order of magnitude or more for Euler and Navier-Stokes calculations; therefore, they must be overcome before complete rotor flow fields can be computed on a routine basis.

The helicoidal vortical wakes of rotor blades have a much larger influence in hover and at low forward speeds than do the trailing vortices of fixed-wing

aircraft. These wakes are complex in geometry and structure, as indicated in figure 10, and treating them accurately and efficiently is perhaps the greatest challenge in helicopter aerodynamics today. Possible special treatments include (1) coupling some form of wake modeling with the finite-difference computations, as
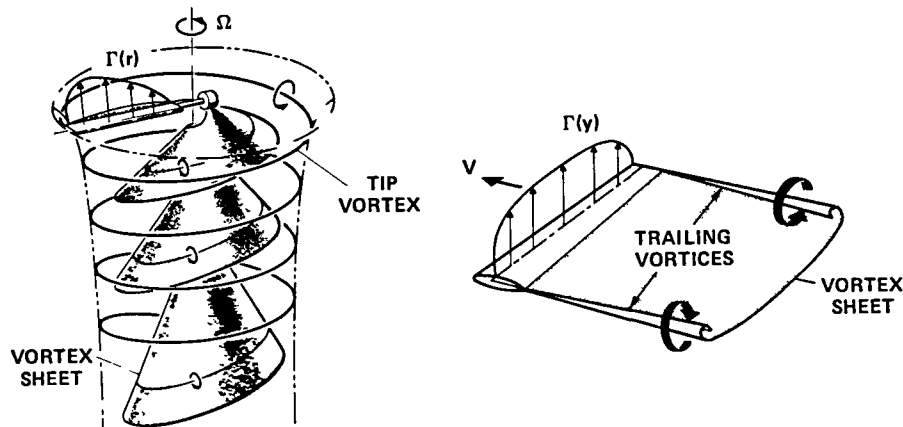

Fig. 10 Schematic of the vortical wakes of a rotor and a wing.

in Refs. 6-9, (2) using three-dimensional extensions of the vortex-fitting ideas as discussed in section III, (3) adapting a refined computational grid to the concentrated vortical regions as they are being computed, (4) developing new vortex-preserving schemes that reduce the inherent numerical dissipation in current codes which rely on vortex capturing, or (5) using combinations of some of these methods.

In addition to the complications of the wake vortices, the geometrical complexity of the computational grids is further compounded when body-fitted grids are considered for the separate rotating and nonrotating components. Fortunately, Rai[20] has recently developed accurate and efficient techniques for interfacing blocks of grids which move relative to one another, as in rotor-stator turbomachinery problems. Figure 11 illustrates a possible arrangement for a simple rotor-body combination, in which a cylindrical grid that rotates with the blades is imbedded into a nonrotating grid that is fitted to the fuselage. Significant reductions in CPU times and memory requirements appear to be attainable if this methodology can be combined with more efficient time-dependent grid-adaption schemes.

Impressive progress in computing three-dimensional rotor flows is evident in references 6-10 and elsewhere, and as a result, more ambitious studies can be expected to surface in the near future. These will include new, full-potential and Euler codes, with specialized Navier-Stokes approaches likely following close behind the Euler codes. However, present limitations of computer speed and memory, algorithm and solution methods, grid generation, vortex modeling, and structural and aerodynamic coupling preclude a finite-difference simulation of the complete flow field about a helicopter in forward flight for the next few years.

The magnitude of the challenge for a fully viscous computation of a meaningful helicopter configuration, such as that shown in figure 11, is indicated by the
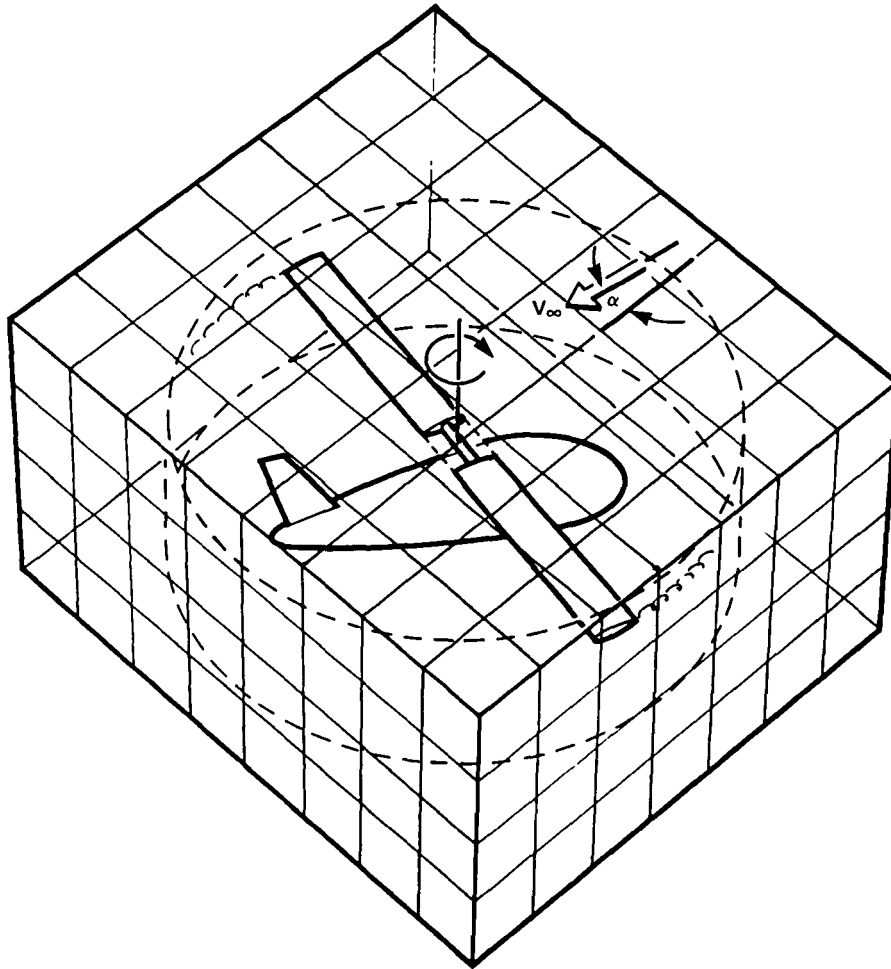
Fig. 11 Schematic of combined moving and fixed computational grids.

following estimates of computational requirements. As noted in reference 19, the CPU time can be estimated from the following formula:

$$CPU = A \times W_{GT} \times N_{G} \times N_{T}/FLOPS \tag{2}$$

where

A = "numerical inefficiency" factor, >1.0

W_{GT} = number floating-point operations per grid point per time-step

N_{G} = number grid points

N_{T} = number time-steps
    = number reference lengths/revolution) $\times$ (number revolutions)/$\Delta\tau$

$\Delta\tau$ = nondiminished time-step

FLOPS = number floating-point arithmetic operations per unit time

For two revolutions of a two-blade rotor in forward flight with blades with an aspect ratio of 10 above a simple fuselage, and for a typical implicit thin-layer Navier-Stokes code with algebraic eddy-viscosity modeling of turbulence, the following values would be (optimistically) appropriate:

$$A = 1.5$$

$$W_{GT} = 4000$$

$$N_G = 10^6$$

$$\Delta\tau = 0.05$$

$$N_T = 2500$$

Then equation (2) yields $CPU \approx 40$ hr for a 100-megaflop supercomputer, or $CPU \approx 4$ hr for a one-gigaflop machine; and approximately 30 million words of memory would be required for this problem. These results suggest that whereas such calculations will at least be feasible in the near future, the megaflop rates of new supercomputers will be more of a limiting factor than memory for practical helicopter aerodynamics.

Finally, another novel aspect of computational methods for helicopter applications is less of a technical issue than a management one; namely, the small number of engineers and research scientists who are skilled in both computational fluid dynamics and in helicopter aerodynamics and dynamics. This factor may well limit the advances in the near future, since to a certain extent, the rate of progress in high-technology fields is proportional to the level of effort being expended, and to the skills of the people who are exerting the effort. In addition, there are even fewer managers who have been trained in both these disciplines, or who appreciate the rapid advances that are occurring in CFD and in supercomputer technology.

V. SUMMARY AND CONCLUSIONS

Existing two-dimensional codes have been found to give reliable and useful information in certain helicopter applications. The most successful example is the prediction of steady section characteristics of rotor airfoils, over a wide range transonic Mach numbers. The basic methodology for incorporating vortex interactions into the finite-difference computations has also been validated, including the prediction of blade airloads and acoustic radiation characteristics. However, the two-dimensional assumption can be a severe limitation in transonic cases with strong

shock waves, and very fine grids appear to be necessary to resolve the acoustic properties of blade-vortex interactions.

Although impressive progress is being made in both two and three dimensions, a finite-difference simulation of the complete flow field about a helicopter in forward flight is not currently feasible. The principal limitations are today's computer speeds and memories, algorithm and solution methods, grid generation, vortex modeling, structural and aerodynamic coupling, and the acute shortage of engineers who are skilled in both computational fluid dynamics and in helicopter aerodynamics and dynamics. Nevertheless, the potential benefits of computational aerodynamics to the helicopter industry are so large that it must take steps to prepare for the next generation of supercomputers.

REFERENCES

1. Johnson, W.: Helicopter Dynamics and Aerodynamics. Princeton University Press, Princeton, New Jersey, 1980.

2. Philippe, J. J.; Roesch, P.; Dequin, A. M.; and Cler, A.: A Survey of Recent Developments in Helicopter Aerodynamics. Paper No. 2, AGARD Lecture Series No. 139, May 1985.

3. McCroskey, W. J.: Special Opportunities in Helicopter Aerodynamics. NASA TM-84396, Dec. 1983.

4. McCroskey, W. J.; Baeder, J. D.; and Bridgeman, J. O.: Calculation of Helicopter Airfoil Characteristics for High Tip-Speed Applications. American Helicopter Society Annual Forum, Ft. Worth, Texas, May 1985.

5. Srinivasan, G. R.; McCroskey, W. J.; and Baeder, J. D.: Aerodynamics of Two-Dimensional Blade-Vortex Interaction. AIAA Paper 85-1560, July 1985.

6. Caradonna, F. X.; and Tung, C.: Finite-Difference Computations of Rotor Loads. NASA TM-86682, 1985.

7. Egolf, T. A.; and Sparks, S. P.: Hovering Rotor Airload Prediction Using a Full Potential Flow Analysis with Realistic Wake Geometry. American Helicopter Society Annual Forum, Ft. Worth, Texas, May 1985.

8. Roberts, T. W.; and Murman, E. M.: Solution Method for Hovering Helicopter Rotor Using the Euler Equations. AIAA Paper 85-0436, Jan. 1985.

9. Cheng, I.-C.; and Tung, C.: Numerical Solution of the Full-Potential Equation for Rotors and Oblique Wings Using a New Wake Model. AIAA Paper 85-0268, Jan. 1985.

10. Desopper, A.: Study of Unsteady Transonic Flow on Rotor Blade with Different Tip Shapes. Paper No. 8, Tenth European Rotorcraft Forum, The Hague, Aug. 1984.

11. Pulliam, T.: Euler and Thin Layer Navier-Stokes Codes ARC2D and ARC3D. Computational Fluid Dynamics User's Workshop, Univ. Tenn. Space Inst. E02-4005-023-84, 1984.

12. Pulliam, T. H.; and Steger, J. L.: Recent Improvements in Efficiency, Accuracy, and Convergence for Implicit Approximate Factorization Algorithms. AIAA Paper 85-0360, Jan. 1985.

13. Baldwin, B. S.; and Lomax, H.: Thin Layer Approximation and Algebraic Model for Separated Turbulent Flows. AIAA Paper 78-257, June 1978.

14. Srinivasan, G. R.: Computations of Two-Dimensional Airfoil-Vortex Interactions. NASA CR-3885, May 1985.

15. Nakahashi, K.; and Deiwert, G. S.: A Self-Adaptive-Grid Method with Application to Airfoil Flow. AIAA Paper 85-1525-CP, July 1985.

16. Caradonna, F. X.; Laub, G. H.; and Tung, C.: An Experimental Investigation of the the Parallel Blade-Vortex Interaction. Paper No. 4, Tenth European Rotorcraft Forum, The Hague, Aug. 1984; also NASA TM-86005, Oct. 1984.

17. George, A. R.; and Chang, S.-B.: Flow Field and Acoustics of Two-Dimensional Transonic Blade-Vortex Interactions. AIAA Paper 84-2309, Oct. 1984.

18. Tijdeman, H.; and Seebass, R.: Transonic Flow Past Oscillating Airfoils. Annual Review of Fluid Mechanics, vol. 12, pp. 181-222, 1980.

19. McCroskey, W. J.; Kutler, P.; and Bridgeman, J. O.: Status and Prospects for Computational Aerodynamics for Unsteady Transonic Viscous Flows. Paper No. 9, AGARD CP-374, Sept. 1984.

20. Rai, M. M.: Navier-Stokes Simulations of Rotor-Stator Interaction Using Patched and Overlaid Grids," AIAA Paper 85-1519-CP, July 1985.

1 Report No NASA TM-86777 USAVSCOM TR-85-A-06	2 Government Accession No	3 Recipient's Catalog No	
4 Title and Subtitle SOME RECENT ADVANCES IN COMPUTATIONAL AERODYNAMICS FOR HELICOPTER APPLICATIONS		5 Report Date October 1985	
		6 Performing Organization Code	
7 Author(s) W. J. McCroskey and J. D. Baeder		8 Performing Organization Report No 85345	
		10 Work Unit No	
9 Performing Organization Name and Address Ames Research Center and Aeroflightdynamics Directorate, U.S. Army Aviation and Technology Activity-AVSCOM, Ames Research Center, Moffett Field, CA 94035		11 Contract or Grant No	
		13 Type of Report and Period Covered Technical Memorandum	
12 Sponsoring Agency Name and Address National Aeronautics and Space Administration, Washington, DC 20546, and U.S. Army Aviation Systems Command, St. Louis, MO 63120		14 Sponsoring Agency Code	

15 Supplementary Notes
Point of Contact: W. J. McCroskey, Ames Research Center, MS 202A-1, Moffett Field, California 94035 FTS 464-6428 or (415) 694-6428

16 Abstract

The growing application of computational aerodynamics to nonlinear helicopter problems is outlined, with particular emphasis on several recent quasi-two-dimensional examples that used the thin-layer Navier-Stokes equations and an eddy-viscosity model to approximate turbulence. Rotor blade section characteristics can now be calculated accurately over a wide range of transonic flow conditions. However, a finite-difference simulation of the complete flow field about a helicopter in forward flight is not currently feasible, despite the impressive progress that is being made in both two and three dimensions. The principal limitations are today's computer speeds and memories, algorithm and solution methods, grid generation, vortex modeling, structural and aerodynamic coupling, and a shortage of engineers who are skilled in both computational fluid dynamics and helicopter aerodynamics and dynamics.

17 Key Words (Suggested by Author(s)) Vortex interaction Helicopter aerodynamics Unsteady transonic flow Computational fluid dynamics	18 Distribution Statement Unlimited Subject Category - 18		
19 Security Classif (of this report) Unclassified	20 Security Classif (of this page) Unclassified	21 No of Pages 18	22 Price* A02

End of Document